

the relativistic wave functions are finite at the origin, the nonrelativistic wave functions currently in use are zero there because of the repulsive nature of the non-relativistic potential at short distances, and in this case one would obtain a form factor going like 2 powers of q^2 faster than the result (7b).

⁹J. Elias *et al.*, Phys. Rev. **177**, 2075 (1969); S. Galster *et al.*, Nucl. Phys. **B32**, 221 (1971); D. Benaksas *et al.*, Phys. Rev. **148**, 1327 (1966).

¹⁰R. J. Reid, Ann. Phys. (N.Y.) **50**, 411 (1968).

¹¹W. W. Buck and F. Gross, Phys. Lett. **63B**, 286 (1976). Briefly, the potential for these models includes only one-pion exchange and a phenomenological approximation to two-pion exchange. The $\lambda_\omega = 1$ model has pure $\gamma^5 \pi NN$ coupling and the combined probability for the two small components is 2.1%.

¹²M. Gari and H. Hyuga, Phys. Rev. Lett. **36**, 345 (1976), and Nucl. Phys. **A264**, 409 (1976).

Threshold Pion Production and Multiplicity in Heavy-Ion Collisions*

P. J. McNulty and G. E. Farrell

Department of Physics, Clarkson College of Technology, Potsdam, New York 13676

and

R. C. Filz

Air Force Geophysics Laboratory, Hanscom Air Force Base, Massachusetts 01731

and

W. Schimmerling† and K. G. Vosburgh‡

Princeton Particle Accelerator, Princeton, New Jersey 08540

(Received 24 April 1977)

Charged pions emerge from roughly 70% of the neon interactions that produce stars in nuclear emulsions at incident energies between 100 and 280 MeV/nucleon. The charged-pion multiplicity averaged 2.8 per pion-producing event. The data are in apparent disagreement with predictions based upon the independent-particle model. Agreement is found with the pion-condensation model of high-density nuclear states as formulated by Kitazoe *et al.*

Nucleus-nucleus interactions are of considerable interest in nuclear and cosmic-ray physics.¹ Of particular importance is the extent to which these interactions differ from predictions of the independent-particle model according to which the interactions are between individual incompressible nucleons in the incident and target nuclei.² To search for possible deviations that would be evidence for such effects as collective phenomena, compression of nuclear matter, shock waves, and pion condensation we have been studying pion production using counter techniques³ and nuclear emulsions.⁴

To the best of our knowledge the emulsion experiment described here (some preliminary results were presented earlier⁴) represents the first study of pions produced in heavy-ion collisions at near threshold incident energies. The number of pion-producing events and the number of pions emerging from the nuclear stars appear to be in substantial disagreement with the predictions of the independent-particle model as formulated by Bertsch² and can be interpreted as evidence for pion condensation of the form de-

scribed by Kitazoe and co-workers.⁵

A stack of 15 Ilford G-5 emulsion pellicles were exposed to a beam of 280-MeV/nucleon neon nuclei at the Princeton particle accelerator. Each pellicle had dimensions of 3 in. \times 4 in. \times 600 μ m. Standard development procedures were followed that normally result in between 15 and 25 blobs along each 100 μ m of trajectory of a relativistic, minimum-ionizing, $Z = 1$ particle. The beam particles entered the stack parallel to the plane of the pellicle and in the absence of strong interactions came to rest about 25 mm into the emulsion. Beam tracks at entrance into the pellicle were examined under a microscope and followed to the location where the neon nucleus came to rest, interacted or left the pellicle. Roughly 20 m of neon track has been followed yielding 189 events.

Since the primary neon nuclei have energies below 280 MeV/nucleon the tracks of energetic pions emerging from interactions are easily distinguished from those of protons or α 's. At these energies it is unlikely that any protons or α 's would emerge from either the incident or target

nucleus with sufficient energy to leave a track that appears as near-minimum ionizing (so-called light tracks). Energetic-charged-pion tracks appear light while proton tracks appear as either gray at the higher energies or black for proton and alpha evaporation prongs. It was, therefore, possible to separate the energetic charged pions by inspection. Light tracks were those that appeared to the scanner to have blob densities of 40 blobs/100 μm or less and gray tracks were those appearing to have between 40 and 60 blobs/100 μm .

To test identifications obtained by inspection, we randomly selected 68 light tracks, which would be identified as pions and measured the blob densities and multiple scattering⁶ along the trajectory. The multiple-scattering measurements yield the product of the momentum, p , and velocity, βc . They were carried out using a Korkiska MS-2 scattering microscope with a 100 \times objective. The momentum could not be obtained from range because the emulsion stack was not thick enough. For comparison 102 gray tracks were also randomly selected for the same measurements.

Figure 1 shows the light (pion) tracks and gray tracks as open and closed circles, respectively, on a plot of blob density versus multiple-scattering measurements of momentum, p , times velocity, βc . The curves in Fig. 1 represent the theoretical relationship⁶ between blob density and $p\beta c$ calculated for pions and protons, assuming that the number of grains ionized along the proton or pion trajectories are proportional to the restricted-energy-loss along the trajectory⁷ as formulated by Sternheimer.⁸ The blob densities

are measured to a statistical accuracy of better than $\pm 5\%$. The values of $p\beta c$, obtained by multiple scattering, are accurate to within 15–20%. Because two or more emulsion grains that overlap are counted as one blob, the exact shape of the theoretical curves depends upon the mean grain diameter.

The curves in Fig. 1 are drawn for mean grain diameters ranging from 0.6 to 0.7 μm which is the range obtained in direct optical measurements made in our laboratory, and are typical of Ilford G-5 emulsions.⁶ The only free parameter for the curves is the proportionality constant between grain density and restricted energy loss.

The curves in Fig. 1 are normalized by blob-density measurements on knock-on electrons (or δ rays) found by scanning along the neon trajectories. The momenta of the scattered electron can be obtained by kinematics from the angle its track makes with the continuation of the neon trajectory and the neon energy as derived from its residual range. The identification of the secondary as an electron and its approximate momentum were confirmed by following the particle to the end of its range or until it began to scatter so wildly that it was no longer possible to follow. Measurements on blob density along 20 knock-on electron trajectories gave values of the proportionality constant that correspond to an average grain density of 18.5 per 100 μm of particle trajectory at minimum ionization.

Figure 1 shows that the curves for pions and protons overlap at low values of $p\beta c$ and cannot be separated by inspection in the region where pions appear gray. At high energies, on the other hand, there appears to be a clear separation between

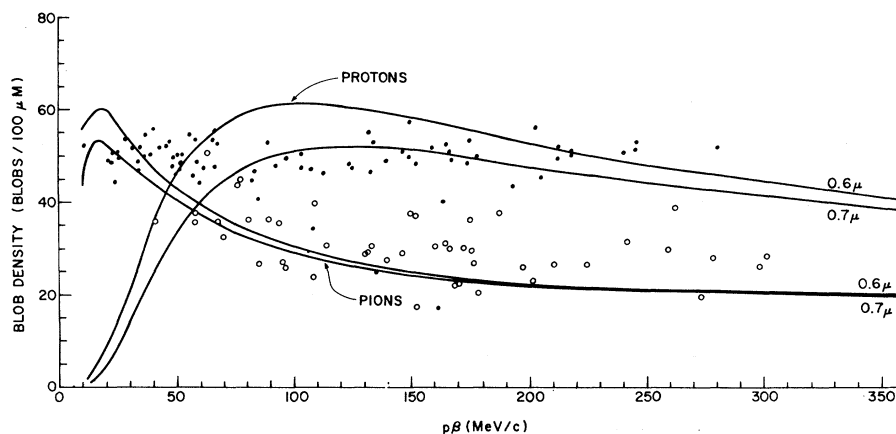


FIG. 1. Blob density vs the product of momentum and velocity for a random sample of tracks. Tracks identified by inspection as light tracks (pions) are represented as open circles and gray tracks (protons) by closed circles.

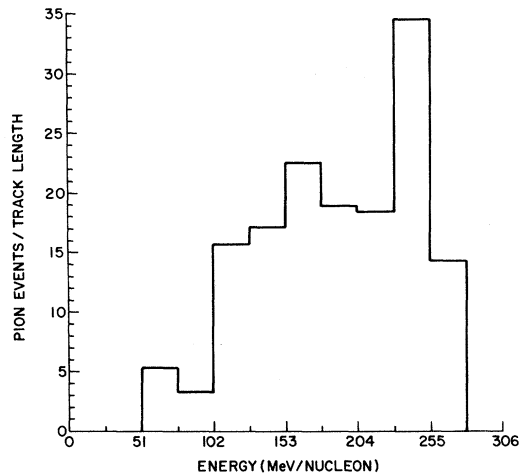


FIG. 2. Production of pions as a function of neon energy.

protons and pions in reasonable agreement with the scanner's identification by inspection. The occasional obvious misidentifications that are evident in Fig. 1 occur either through a mistaken labeling or a steep light track appearing gray. The data of Fig. 1 have been corrected for dip angle.

The relative number of events with light tracks emerging per unit length of track scanned is plotted in Fig. 2 versus the neon energy as determined from the event's distance upstream from the neon end of range. There is a sharp rise in pion production at a neon energy of about 100 MeV/nucleon.

Bertsch² has recently analyzed pion production for O^{16} incident on U^{238} nuclei under the most economical assumptions, in particular, with no collective effects at all. The model can, therefore, be used as a baseline for analyzing experimental data. Serious discrepancies (which Bertsch suggest should be order of magnitude) would indicate collective effects. According to Bertsch there is enough relative Fermi momentum between nucleons on the colliding nuclei to produce pions at incident heavy-ion energies as low as 54 MeV/nucleon which is consistent with the neon data plotted in Fig. 1 where the lowest-energy pion event in this experiment occurred at 67 MeV/nucleon.

According to Bertsch's model, the fraction of events from which pions emerge should increase from $\frac{1}{3000}$ at threshold to $\frac{1}{27}$ at 250 MeV/nucleon if collective effects are ignored. This is not consistent with our data where about 70% of events

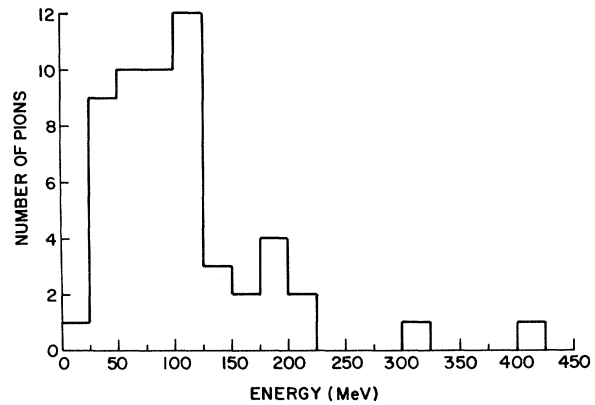


FIG. 3. Pion energy spectrum in the laboratory frame.

between 100 and 280 MeV/nucleon have charged pions emerging. Bertsch's model also strongly implies single-pion production in this energy range because the initially high Fermi momentum distributions are expected to quickly thermalize as the collision progresses. The experimentally observed average number of pions to emerge from a pion event is 2.8. Thus, our findings are inconsistent with Bertsch's assumptions.

Kitazoe and co-workers⁵ have used the hydrodynamic model to include the collective effects on the formation of high-density states in nuclear matter in heavy-ion collisions. In particular they explored the effect of pion production on the formation of high-temperature and high-density matter. Their analysis suggests that the condensation of zero-momentum pions will be appreciable at incident energies of 120–440 MeV/nucleon, reaching a peak production at an incident energy of about 220 MeV/nucleon. Production of zero- and higher-momentum pions is expected to reach as high as 0.4 pions per nucleon and if roughly $\frac{1}{3}$ emerge from the nucleus then according to Fig. 1(b) of Ref. 5, there would be a sharp rise in pion production to 2–5 pions per event with a peak at about 220 MeV/nucleon which is in agreement with the data of Fig. 2.

The energy spectrum in the laboratory frame of a random selection of light tracks identified as pions is shown in Fig. 3. Pions at energies below 50 MeV in the laboratory frame would not appear as light tracks according to Fig. 1 and would, therefore, not be included in Fig. 3. The energy spectrum agrees with the independent-particle-model calculations of Bertsch. Pions at lower energies, however, would not be detected in this experiment and it is not clear that any collective

phenomena suggested to date^{1,5} would predict pions at significantly higher energies. In particular, the condensation pions of Kitazoe and co-workers⁵ should also emerge with low energies. The pion energy spectra may in fact provide information on the thermal state of the shock wave.

We would like to thank Professor M. White for giving us beam time during the final days of the Princeton particle accelerator and the Fannie Rippel Foundation for supporting the accelerator during that period.

*Supported in part by Air Force Contract No. F19628-C-02-9 to Clarkson College of Technology and No. F19628-73-C-0190 to Emmanuel College.

†Presently at Lawrence Berkeley Laboratory, Berkeley, Calif. 94720.

‡Presently at General Electric Research and Development Center, Schenectady, N. Y. 12230.

¹R. F. Sawyer and D. J. Scalapino, Phys. Rev. D **7**, 953 (1972); W. Scheid, H. Muller, and W. Greiner, Phys. Rev. Lett. **32**, 74 (1974); A. A. Amsden, G. F. Bertsch, F. H. Harlow, and J. R. Nix, Phys. Rev. Lett. **35**, 905 (1975); M. I. Sobel, P. J. Siemens, J. P. Band-

orf, and H. A. Bethe, Nucl. Phys. **A251**, 502 (1975); A. Abul-Madg, J. Hufner, and B. Schurmann, Phys. Lett. **60B**, 327 (1976); H. G. Baumgardt, J. U. Schott, Y. Sakamoto, E. Schopper, H. Stocker, J. Hofman, W. Schied, and W. Greiner, Z. Phys. **A273**, 359 (1971); H. Heckman, D. C. Greiner, P. J. Lindstrom, and F. S. Bieser, Science **174**, 1130 (1971); H. J. Crawford, P. B. Price, J. Stevenson, and L. W. Wilson, Phys. Rev. Lett. **34**, 329 (1975); T. D. Lee, and G. C. Wick, Phys. Rev. D **9**, 2291 (1974); V. Ruck, M. Gyulassy, and W. Greiner, Z. Phys. **A277**, 391 (1976).

²G. F. Bertsch, Phys. Rev. C **15**, 713 (1977).

³W. Schimmerling, K. G. Vosburgh, K. Koepke, and W. D. Wales, Phys. Rev. Lett. **33**, 1170 (1974), and Phys. Rev. D **111**, 1743 (1975).

⁴P. J. McNulty and R. C. Filz, in *Proceedings of the Eighth International Conference on Nuclear Photography and Solid State Track Detectors*, edited by M. Nicolae (Institute of Atomic Physics, Bucharest, 1972), Vol. 2, p. 170.

⁵Y. Kitazoe, M. Sano, and H. Tok, Lett. Nuovo Cimento **13**, 139 (1975); Y. Kitazoe and M. Sano, Lett. Nuovo Cimento **14**, 400, 407 (1975).

⁶W. H. Barkas, *Nuclear Research Emulsions* (Academic, New York, 1963).

⁷P. J. McNulty and F. J. Congel, Phys. Rev. D **1**, 3041 (1970).

⁸R. M. Sternheimer, Phys. Rev. **164**, 349 (1967).

Photoelectron Angular Distributions of *s* Electrons in Open-Shell Atoms

Anthony F. Starace*†

Behlen Laboratory of Physics, The University of Nebraska, Lincoln, Nebraska 68588

and

Robert H. Rast‡§ and Steven T. Manson‡

Department of Physics, Georgia State University, Atlanta, Georgia 30303

(Received 16 May 1977)

It is shown that the photoelectron angular distribution of *s* electrons in an open-shell atom, having outer configuration ns^2np^a , is not described by the asymmetry parameter $\beta=2$, as predicted by more approximate theories, but has dramatic variations with energy even within *LS* coupling. Calculations for the 3*s* subshell in Cl are presented as an example.

One of the most striking predictions of the photoelectron angular distribution theory of Cooper and Zare¹ is that photoionization of an electron having orbital angular momentum $l=0$ leads to a pure $\cos^2\theta$ photoelectron angular distribution, irrespective of the photon's energy. Here θ is measured from the axis of linear polarization of the incident light and the differential cross section is

$$d\sigma/d\Omega = (\sigma/4\pi)[1 + \beta P_2(\cos\theta)].$$

A pure $\cos^2\theta$ distribution corresponds to an asymmetry parameter $\beta=2$. Classically, this result is intuitively obvious: Since the initial state is spherically symmetric, the photoelectron angular distribution is centered about the electric vector of the incident light. Quantum mechanically, with neglect of retardation and relativistic effects, this result holds exactly for photoionization of atomic hydrogen.² For more complicated atoms, this result follows in the Cooper-Zare theory¹ from the approximation that in the final state